Improved Reliability of Single-Phase PV Inverters by Limiting the Maximum Feed-in Power

Yang, Yongheng; Wang, Huai; Blaabjerg, Frede

Published in:
Proceedings of the 2014 IEEE Energy Conversion Congress and Exposition (ECCE)

DOI (link to publication from Publisher):
10.1109/ECCE.2014.6953385

Publication date:
2014

Document Version
Early version, also known as pre-print

Digital Object Identifier (DOI):

Proceedings of the IEEE Energy Conversion Congress and Exposition (ECCE 2014), Pittsburgh, PA, USA, 14-18 September, 2014.

Improved Reliability of Single-Phase PV Inverters by Limiting the Maximum Feed-in Power

Yongheng Yang
Huai Wang
Frede Blaabjerg

Suggested Citation

Y. Yang, H. Wang, and F. Blaabjerg, "Improved reliability of single-phase PV inverters by limiting the maximum feed-in power," *in Proc. IEEE Energy Convers. Congr. and Expo.*, 2014, pp. 128-135.

Improved Reliability of Single-Phase PV Inverters by Limiting the Maximum Feed-in Power

Yongheng Yang, *IEEE Student Member*, Huai Wang, *IEEE Member*, Frede Blaabjerg, *IEEE Fellow*
Department of Energy Technology
Aalborg University
Pontoppidanstraede 101, Aalborg East DK-9220, Denmark
yoy@et.aau.dk, hwa@et.aau.dk, fbl@et.aau.dk

***Abstract*— Grid operation experiences have revealed the necessity to limit the maximum feed-in power from PV inverter systems under a high penetration scenario in order to avoid voltage and frequency instability issues. A Constant Power Generation (CPG) control method has been proposed at the inverter level. The CPG control strategy is activated only when the DC input power from PV panels exceeds a specific power limit. It enables to limit the maximum feed-in power to the electric grids and also to improve the utilization of PV inverters. As a further study, this paper investigates the reliability performance of the power devices (e.g. IGBTs) used in PV inverters with the CPG control under different feed-in power limits. A long-term mission profile (i.e. solar irradiance and ambient temperature) based stress analysis approach is extended and applied to obtain the yearly electrical and thermal stresses of the power devices, allowing a quantitative prediction of the power device lifetime. A study case on a 3 kW single-phase PV inverter has demonstrated the advantages of the CPG control in terms of improved reliability.**

I. Introduction

With a spectacular growth rate of PhotoVoltaic (PV) installations, challenging issues like overloading of the grid due to the peak power generation of PV systems have recently gained much attention [1]–[3]. In the case of a very large-scale adoption of PV systems, advanced control strategies like power-ramp limitation and absolute power control, which are currently e.g. required for wind power systems in Denmark, should also be transitioned and strengthened into the next-generation PV systems [1], [4]–[9]. As a power limiting control, a Constant Power Generation (CPG) control by limiting maximum feed-in power has been proposed in [9], and witnessed as an effective way to eliminate overloading. When it is compared to the solutions of expanding the power grid infrastructure or integrating energy storage systems to tolerate the peak power [4]–[11], the CPG control might be a more economically viable strategy, since it only contributes to a limited energy yield reduction in a real case, where typically the peak power generation is very rare.

In addition, the CPG control allows a reduction of the thermal stresses on the power devices (e.g. IGBTs), since the power losses inducing temperature rises inside the power devices will be changed, when the PV system enters into CPG mode from Maximum Power Point Tracking (MPPT) mode and vice versa. As a consequence, the thermal stresses will affect the reliability of the PV system. However, there is still a lack of quantitative analysis on the potential reliability improvement enabled by the CPG control, besides the mitigation of overloading at a high penetration level. Moreover, even for real-field applications, where limiting peak power control was not initially included, the CPG control can still be applied for potentially extending the lifetime of existing PV inverters by only software algorithm modifications. Seen from this point, it is interesting to justify the long-term performance of PV inverters from both reliability and economic viability (i.e. a trade-off between the lifetime extension and the overall energy yield reduction), and thus find the optimal power limitation level in terms of cost-of-energy [4], [9], [11].

Regarding the reliability of PV inverters, it has become of intense importance and involves multiple disciplines [5], [7], [12]–[19]. The lifetime prediction research on power devices is transitioning from handbook-based approaches [18], [19] to more physics-based methods, which require in-depth understanding of various failure mechanisms and thus dedicated lifetime models, e.g. an analytical based Confin-Mason model [12]–[14], [16]. Among these failure factors, thermal stresses, depending on the mission profile as well as the inverter operating conditions, have been the most observed ones in PV systems (both inverters and capacitors) [17], [20]. Hence, the varying operation conditions due to the intermittent nature of solar energy has been one of the challenges to perform reliability analysis in PV systems. Currently, most of the existing reliability prediction methods for the lifetime estimation of power devices in PV inverters only consider either short-term mission profiles [13], [14] or long-term mission profiles with a low data-sampling frequency, where the effects of small temperature cycles are not considered [19]. Moreover, the widely used lifetime models unfortunately consider only a few failure modes, e.g. the junction temperature cycle amplitude and the mean junction temperature [16], [19]–[22]. However, improving the lifetime estimation accuracy requires an elaborated analysis of a long-term mission profile, and also a detailed reliability model.

In view of the above issues, a mission profile based reliability analysis approach has been proposed in [17], which is extended and applied to the PV systems with the MPPT-CPG control in this paper. This reliability approach takes a real-field yearly mission profile with a high sampling rate

978-1-4799-5776-7/14/$31.00

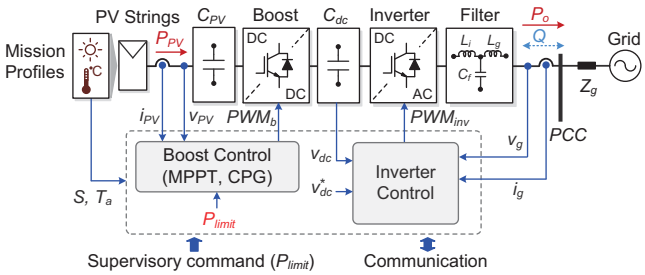

Fig. 1. A two-stage single-phase grid-connected PV system with MPPT and CPG control considering mission profiles.

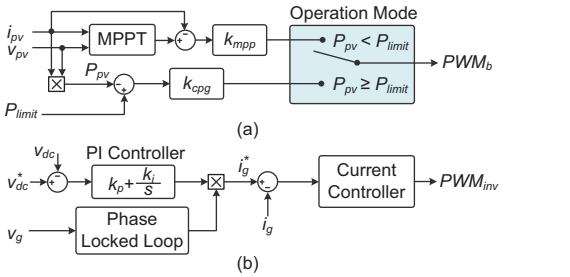

Fig. 2. Control diagram of a single-phase PV system with CPG ability: (a) boost control diagram and (b) PV inverter control system.

(200 ms) into consideration, and the mission profile has been decomposed into the ones of different time scales, i.e. short-term mission profiles and long-term mission profiles. The resultant mission profile at a large time scale is analyzed using a rain-flow counting algorithm. The MPPT-CPG control method has been applied to a 3 kW single-phase PV system. The temperature loading profiles, including thermal cycles at fundamental frequency induced by short-term mission profiles and the cycles with large periods mainly due to long-term mission profiles, offer the possibility to quantitatively calculate the consumed life and thus an estimation of the lifetime with a reliability model. The application of the extended reliability analysis approach presented in § III shows that, a PV system with CPG control, which only leads to a limited energy yield reduction, can contribute not only to unloading of the grid but also to improved reliability of the power converters.

II. System Description and Operation

The PV system considered in this paper is a single-phase system as shown in Fig. 1. The boost converter offers the flexibilities of MPPT and active power control (e.g. CPG control) [9], and extends the operational time of the PV inverter when the solar irradiance level is very low. The PV inverter can be transformerless to maintain a high efficiency. In this paper, a full-bridge topology with a bipolar modulation scheme is adopted, since the bipolar modulation scheme can effectively mitigate leakage currents, which is required by PV integration standards. A hybrid control scheme of MPPT and CPG control allows further to increase the penetration level. The CPG control can be implemented by a) integrating energy storage systems like a battery, b) managing the power at the secondary control level, and c) modifying the conventional MPPT algorithms [4], [8], [9].

The CPG control by modifying the MPPT algorithm is adopted in this paper for the single-phase PV systems due to its simplicity. The control structure of a two-stage PV system with the CPG control is shown in Fig. 2. The operation principle of a PV system with the MPPT-CPG hybrid control scheme can be described as follows. When the available PV output power P_{PV} exceeds the power limitation P_{limit}, the system goes into the CPG mode with a constant power generation of the PV strings, which is controlled by a proportional controller (k_{cpg}). When $P_{PV} \leq P_{limit}$, the PV system operates in MPPT mode

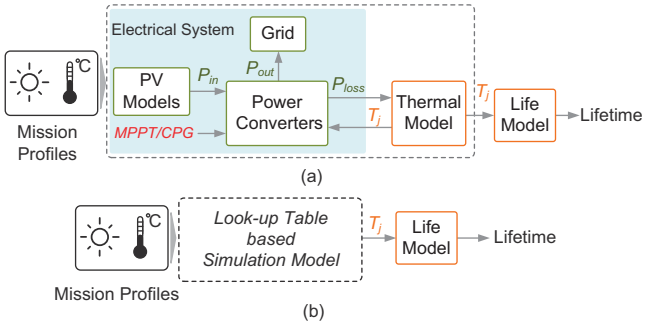

Fig. 3. Mission profile based lifetime analysis approach for the power switching devices: (a) detailed structure for short-term mission profiles and (b) look-up table based analysis structure for long-term mission profiles.

with a peak power injection to the grid from the PV strings. A proportional controller k_{mpp} is used to regulate the PV panel current. It can be seen that the hybrid control scheme requires minor and simple control algorithm modifications instead of complicated hardware adjustments (e.g. with energy storage systems), which means that it does not increase the total implementation cost. In respect to the current controller, a good power quality of the injected grid current should be maintained in terms of low total harmonic distortions [23]. Considering this issue, a Proportional Resonant (PR) controller [23], [24] has been adopted as the current controller in Fig. 2. In both operation modes, the DC-link voltage v_{dc} is controlled through a Proportional Integrator (PI) controller to follow the reference command, v_{dc}^*.

III. Mission Profile Based Reliability Analysis

Improving the reliability of the power electronics based PV system has been an intense topic [25] in order to integrate cost-effective solar PV energy into the grid. The mission profile has been witnessed as one determining factor of the failure in power converters [19], [20], [26], [27]. Thus, a mission profile based lifetime analysis approach [17] is extended in the following section considering both short-term and long-term mission profile effects.

A. Mission Profile based Lifetime Analysis Approach

Fig. 3 shows the extended mission profile based reliability analysis approach. This reliability analysis approach can be

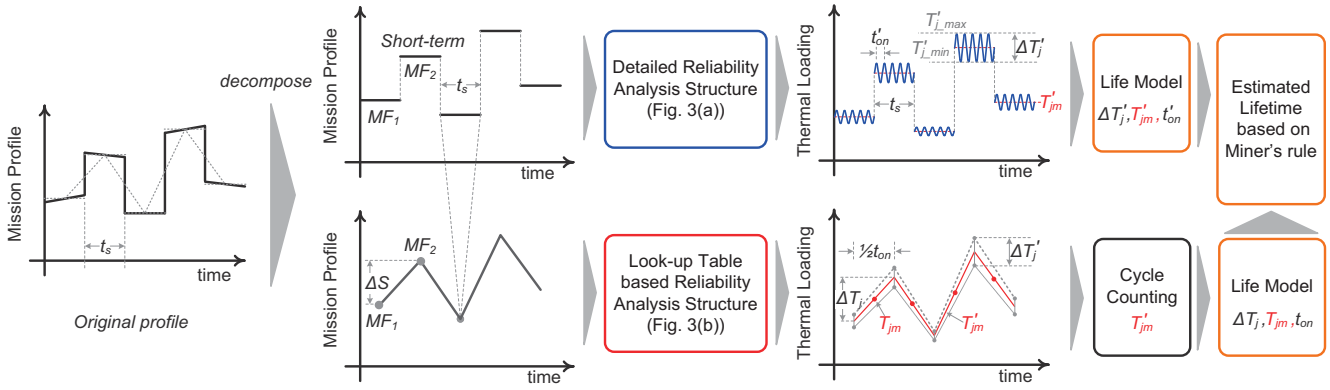

Fig. 4. Proposed mission profile decomposition procedure of the extended reliability analysis approach for temperature loading translation.

adopted for analysis of mission profiles at different time scales, and thus predict the lifetime of IGBTs. For short-term mission profiles, the temperature loading profile (junction temperature) can directly be obtained from Fig. 3(a). However, for a long-term mission profile with a high data-sampling rate (e.g. 200 ms), it will be time-consuming, or even impossible, to capture the full temperature loading profile. Thus, look-up tables are adopted to accelerate the evaluation process as it is shown in Fig. 3(b), which requires decomposing the mission profile at different time scales.

A decomposition procedure is proposed as shown in Fig. 4, where the original mission profile is decomposed with a period of t_s under an assumption that in this short period the mission profile of t_s is constant and that the junction temperature can go into steady state within the time of t_s. Consequently, in each time interval of t_s, the mission profile (e.g. MF_1 and MF_2) can be treated as a short-term mission profile, where the analysis approach shown in Fig. 3(a) is applicable. Notably, under the decomposed short-term mission profile, the thermal cycles are mainly at fundamental frequency with identical cycle period, $t_{on}^{'}$, e.g. $t_{on}^{'} = 0.02$ s in a 50 Hz power grid, as exemplified in Fig. 5. However, as it is shown in Fig. 4, there is a stress difference (e.g. the stress difference ΔS between MF_1 and MF_2) among those short-term mission profiles, and this will also introduce temperature stresses on the power devices, as shown in Fig. 5. Therefore, a long-term mission profile is reconstructed using the average stress from short-term mission profiles (e.g. MF_1 and MF_2). Finally, a look-up table based approach shown in Fig. 3(b) can be applied to extract the long-term thermal loading profile.

B. Temperature Loading Interpretation

After the decomposition of the long-term mission profile, the temperature loading profiles appearing in the power devices should be appropriately extracted or interpreted according to the lifetime model. For example, the Coffin-Manson model [12]–[14], [22] indicates that the number of cycles to failure (N_f) is only dependent on the temperature cycles, including cycle amplitude (ΔT_j) and mean junction temperature (T_{jm}). Those values can be obtained under a short-term

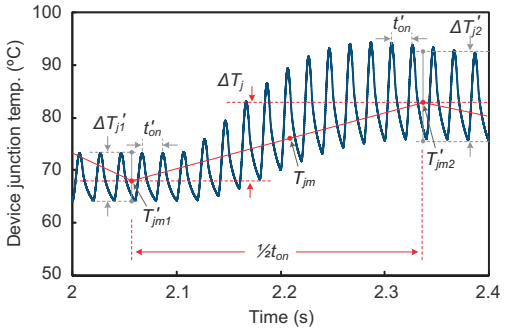

Fig. 5. Temperature loading example of the power devices in the case of solar irradiance variations ($T_a = 50$ °C).

mission profile, as it is shown in Fig. 3(a) and Fig. 4, while for a long-term mission profile, counting algorithms are used to extract the temperature loading profile information. There are many cycle counting algorithms reported, e.g. level crossing counting, rain-flow counting, and simple range counting methods [13]–[15], [26], which can be used to appropriately interpret the thermal loading profile according to a dedicated lifetime model. Then, the lifetime can be calculated with the extracted information. However, it has been found that N_f is also affected by the cycle period (t_{on}), bond-wire aspect ratio (ar), and the diode (f_d) [21]. Hence, a detailed lifetime model has been introduced in [21], and it can be given by,

$$N_f = A\Delta T_j^{\alpha}(ar)^{\beta_1 \Delta T_j + \beta_0} f(t_{on}) \exp\left(\frac{E_a}{k_B T_{jm}}\right) f_d \quad (1)$$

with

$$f(t_{on}) = \frac{C + (t_{on})^{\gamma}}{C+1}$$

in which A, α, β_0, β_1, γ and C are the model parameters that can be obtained by means of curve-fitting using numerical simulation or experimental results (accelerating tests) [16]. k_B is the Boltzmann constant, and E_a is the activation energy. The values of those parameters and also the test conditions for an IGBT module are shown in Table I.

TABLE I

PARAMETERS OF THE LIFETIME MODEL OF AN IGBT MODULE [21].

Parameter	Value	Unit	Experimental condition
A	3.4368 $\times 10^{14}$	-	
α	-4.923	-	64 K $\leq \Delta T_j \leq$ 113 K
β_1	-9.012 $\times 10^{-3}$	-	0.19 $\leq ar \leq$ 0.42
β_0	1.942	-	
C	1.434	-	0.07 s $\leq t_{on} \leq$ 63 s
γ	-1.208	-	
f_d	0.6204	-	
E_a	0.06606	eV	32.5 °C $\leq T_{jm} \leq$ 122 °C
k_B	8.6173324$\times 10^{-5}$	eV/K	

According to the Miner's rule [12]–[15], the accumulated Life Consumption LC (i.e. damage to the device) is linearly dependent on the contributions from different temperature cycles, which can be expressed as,

$$LC = \sum_i \frac{n_i}{N_{fi}} \tag{2}$$

where n_i is the number of cycles at the stress ΔT_{ji} and N_{fi} is the corresponding number of cycles to fail according to (1). Then, the lifetime of the power devices (LF) can quantitatively be calculated as $LF = T_{mp}/LC$ under the mission profile with a duration of T_{mp}.

Although a counting algorithm can enable a quantitative interpretation of the power device loading, the limitations remain in the analysis. For example, as shown in Table I, the parameters of the lifetime model (1) are extracted under specific conditions (e.g. 0.07 s $\leq t_{on} \leq$ 63 s) for a certain power device, and thus they are not very feasible to use for a quantitative calculation of the lifetime of the power devices used in this paper. However, a qualitative reliability comparison of the power devices in the PV inverter in different operation modes (with or without CPG control) can still be enabled by normalizing the LC so that the parameter dependency is reduced. The LC normalization can be expressed as,

$$\overline{LC} = \frac{LC_c}{LC_p} = \frac{\sum_i \frac{n_i}{(\Delta T_{ji})^{\alpha}(ar)^{\beta_1 \Delta T_{ji}}[C+(t_{oni})^{\gamma}]\exp(\frac{E_a}{k_B T_{jmi}})}}{\sum_l \frac{n'_l}{(\Delta T'_{jl})^{\alpha}(ar)^{\beta_1 \Delta T'_{jl}}[C+(t'_{onl})^{\gamma}]\exp(\frac{E_a}{k_B T'_{jml}})}} \tag{3}$$

in which $\overline{LC}$ is the normalized life consumption, LC_p is the base LC for normalization (i.e. the LC of the power devices of the PV inverter without CPG control under a mission profile), LC_c is the LC of the power devices under the same mission profile, n_i, n'_l are the number of cycles at the stress ΔT_{ji} and $\Delta T'_{jl}$, respectively, and α, β_1, γ, C, k_B, and E_a are the lifetime model parameters listed in Table I.

According to (3), the LC of the power devices of the PV inverter in different operation modes can be qualitatively compared, and thus the lifetime can be given as,

$$LF_c = \frac{1}{\overline{LC}} LF_p \tag{4}$$

with LF_c and LF_p being the lifetime of the power devices in the PV inverter with CPG and without CPG control (i.e. only MPPT control), respectively.

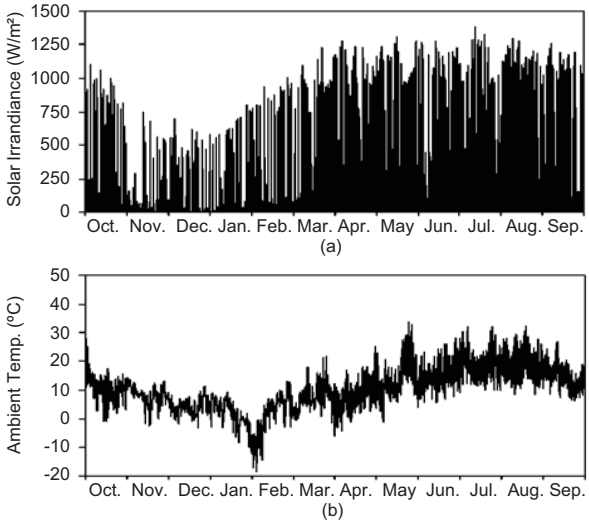

Fig. 6. A yearly real-field mission profile (200 ms sampling rate): (a) solar irradiance level and (b) ambient temperature.

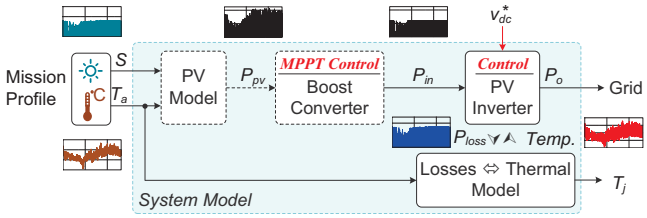

Fig. 7. Power flow diagram (simulation model) of a single-phase PV system with MPPT control under a modified mission profile to emulate the thermal loading profile when the CPG control is applied.

IV. SIMULATION AND EXPERIMENTS

A. Simulation Results

In order to verify the extended reliability analysis approach and also the effectiveness of limiting the maximum feed-in power in terms of reliability improvement, referring to Fig. 1 and Fig. 2, a single-phase 3 kW PV inverter is studied with the mission profile shown in Fig. 6 by simulations. According to Fig. 4, the mission profile has been decomposed with a frequency of 1 Hz (t_s = 1s). In the MPPT-CPG operation mode, the solar irradiance profile is reconstructed in order to achieve constant power generation, as illustrated in Fig. 7. The PV strings consist of 45 PV panels (15 in each string), and the parameters of the PV panel is shown in Table II. The other parameters of the PV system are listed in Table III.

TABLE II

PARAMETERS OF A SOLAR PV PANEL

Parameter	Symbol	Value	Unit
Rated power	P_{mpp}	65	W
Voltage at P_{mpp}	V_{mpp}	17.6	V
Current at P_{mpp}	I_{mpp}	3.69	A
Open circuit voltage	V_{OC}	21.7	V
Short circuit current	I_{SC}	3.99	A

TABLE III

PARAMETERS OF THE TWO-STAGE SINGLE-PHASE PV SYSTEM.

Parameter	Value
Boost converter inductor	$L_1 = 5$ mH
DC-link capacitor	$C_{dc} = 2200$ μF
PV-side capacitor	$C_{PV} = 220$ μF
	$L_i = 2$ mH - inverter-side inductor
LCL-filter	$L_g = 3$ mH - grid-side inductor
	$C_f = 4.7$ μF - capacitor
Damping resistor of *LCL*-filter	$R_d = 10$ Ω
Switching frequencies	$f_b = f_{inv} = 10$ kHz
MPPT sampling frequency	$f_{mppt} = 100$ Hz
Grid nominal voltage (RMS)	$V_g = 230$ V
Grid nominal frequency	$\omega_0 = 2\pi \times 50$ rad/s

As aforementioned, a PI controller $G_{DC}(s)$ is adopted to control the DC-link voltage to be $v_{dc}^* = 400$ V and a PR controller with resonant Harmonic Compensators (HC) has been used as the current controller $G_C(s)$ to ensure the power quality of the injected grid current. Those controllers can be expressed as,

$$G_{DC}(s) = k_{pp} + \frac{k_{ip}}{s} \tag{5}$$

$$G_C(s) = \overbrace{k_{pr} + \frac{k_{ir}}{s^2 + \omega_0^2}}^{PR} + \overbrace{\sum_{h=3,5,7} \frac{k_{ih}}{s^2 + (h\omega_0)^2}}^{HC} \tag{6}$$

with ω_0 being the fundamental grid frequency and h being the harmonic order. The parameters of these controllers are given in Table IV. The thermal loading of the power devices under the decomposed yearly real-field mission profile is presented in Fig. 8, where the feed-in power is limited to 80 % of the peak power in the hybrid MPPT-CPG operation mode. As it is shown in Fig. 8, the maximum junction temperature of the device has been reduced by 9 °C under the decomposed mission profile, when the feed-in power is limited to 80 % of the peak power. Consequently, a qualitative conclusion can be drawn that limiting the maximum feed-in power (i.e. MPPT-CPG operation mode) will contribute to an improved reliability of the power switching devices.

In order to get a quantitative comparison of the lifetime improvement enabled by the MPPT-CPG control, a rain-flow counting algorithm has been used to extract the temperature stress information from the loading profile shown in Fig. 8. The number of cycles of those loading profiles are shown in Fig. 9. According to the lifetime model in (1) and also (2), the consumed life can be calculated, and thus the lifetime under the given mission profile. As it is shown in Fig. 9, with the hybrid MPPT-CPG control of 20 % power reduction, the number of cycles of the temperature cycling amplitudes ΔT_j from 15 °C to 65 °C has been reduced significantly, and the number of cycles of the mean junction temperatures ΔT_{jm} within a range of 35 °C $\sim$ 65 °C is also clearly reduced. In accordance to (1) and (2), both the increase of the number of cycles to fail N_f (mainly due to lower T_{jm}) and the reduction of the number of cycles n_i will contribute to a decrease of the accumulated life consumption, and thus an improved reliability

TABLE IV

CONTROLLER PARAMETERS FOR THE SINGLE-PHASE SYSTEM.

Parameter	Value
MPPT control gain	$k_{mpp} = 23.8$
CPG control gain	$k_{cpg} = 2$
DC-link (PI) controller	$k_{pp} = 0.1$, $k_{ip} = 1.25$
PR controller	$k_{pr} = 8$, $k_{ir} = 2000$
Harmonic compensator	$k_{i3,i5,i7}$= 1500

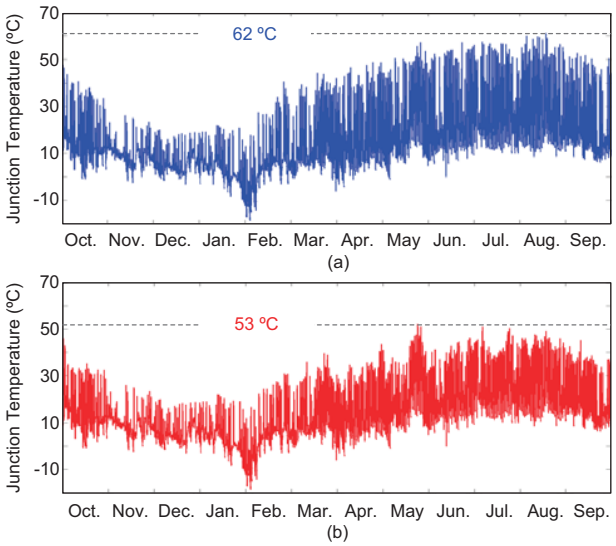

Fig. 8. Thermal loading of the power devices in a 3 kW PV inverter (a) with MPPT control and (b) with 80 % feed-in of the peak power in MPPT-CPG mode.

of the power devices of the PV inverter under this mission profile has been achieved.

Notably, when applying the rain-flow counting to the life-time model of (1), the confidence level of the resultant device reliability is dependent on the model parameters (e.g. due to specific test conditions). To reduce the parameter dependency, the counting results of the thermal loading profiles are applied to the normalized LC model given by (3), and thus a reasonable comparison of high confidence can be done as shown in Fig. 10. It can be seen in Fig. 10(a) that the temperature cycles within a range of 15 °C to 55 °C consumed the most of the life under the decomposed long-term mission profile. Moreover, although the temperature cycles with large amplitudes (e.g. 45 °C $< \Delta T_j <$ 55 °C) account for a small number, they have contributed to much loading. One conclusion drawn from Fig. 10(b) is that temperature cycles with the periods of 1 min to 1 hour are the main contributors of the device damage (i.e. the most life consuming loading) under the decomposed long-term mission profile. In fact, the real-field mission profile varies at a rate of minutes, which means that the previous assumption for the mission profile decomposition is reasonable, and thus the temperature cycles within this range consume much lifetime. Nevertheless, the above results have verified the reliability benefit of limiting the maximum feed-in power control besides unloading the distributed grid.

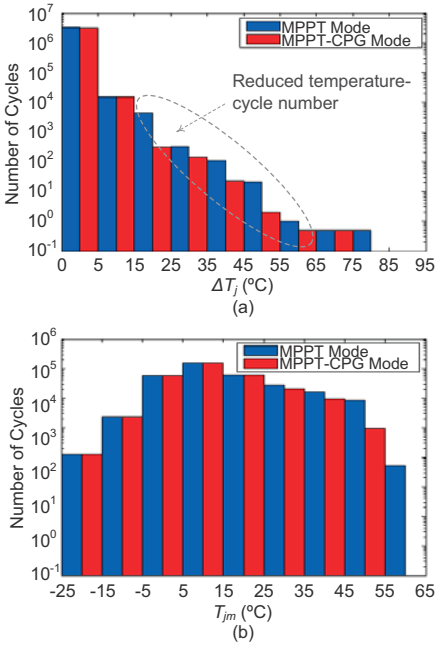

Fig. 9. Rain-flow counting results of the thermal loading profile shown in Fig. 8 for the power devices of a 3 kW single-phase PV inverter in different operation modes (MPPT and MPPT-CPG with 80 % of peak power feed-in): (a) junction temperature cycling amplitude ΔT_j and (b) mean junction temperature T_{jm}.

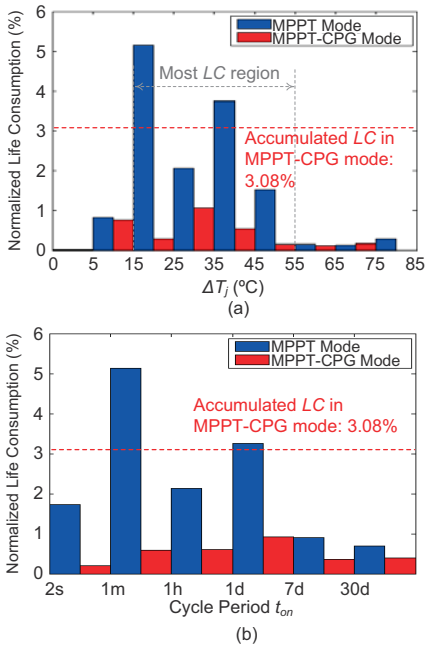

Fig. 10. Normalized life consumption of the power device of a 3 kW single-phase PV inverter considering the loading profiles shown in Fig. 6 in different operation modes (MPPT and CPG with 80 % of peak power feed-in): (a) normalized life consumption distribution on ΔT_j and (b) normalized life consumption distribution on the cycle period t_{on}.

In order to further investigate the benefits of reliability improvement by limiting the maximum feed-in power of PV systems, more evaluations have been carried out on the same system. The results are shown in Fig. 11. It can be observed from Fig. 11 that, with a certain reduction (e.g. 10 % or 20 %) of the feed-in power from PV systems, the annual energy yield reduction is quite limited (e.g. 3.11 % or 6.23 %), while the accumulated damage (LC) under this mission profile has been reduced (65.0 % or 82.2 % respectively), and thus the reliability of the power devices is improved significantly. Fig. 11 also demonstrated the feasibility of the MPPT-CPG control due to its limited energy reduction through a long-term operation. Those evaluations have further verified the effectiveness of reliability improvement by limiting the maximum feed-in power to the grid. A worthy point to make is that a trade-off between the lifetime extension and the yearly energy generation have to be taken into account. Fig. 11 offers the possibility for the 3 kW PV inverters under the specific mission profile given in Fig. 6 to optimize its energy production and the thermal performance of the power devices in order to reduce the cost of energy. For different applications, an appropriate power limit is closely dependent on the trade-off between lifetime improvement and energy reduction, as well as the customer demands for expected lifetime of the inverters. Nonetheless, the extended reliability analysis method can be adopted to enhance the design and operation phases of the PV inverter systems. In addition, it should be mentioned that the reliability analysis introduced in this paper is just about one power device in a PV inverter. The lifetime estimation

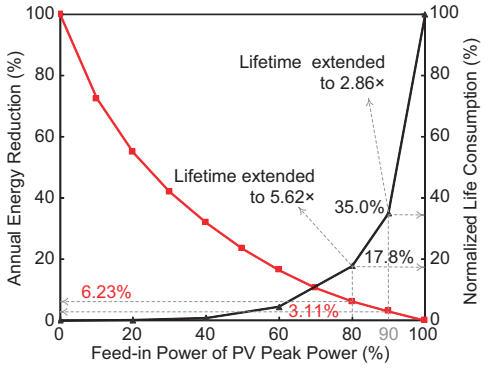

Fig. 11. Energy reduction and normalized life consumption of the power devices due to the limitation of maximum feed-in power considering the mission profile shown in Fig. 6 for a 3 kW PV inverter system.

of the entire PV inverter and even the whole PV system requires an in-depth knowledge of multiple subjects, since the components (e.g. capacitors and inverters) in the PV systems have cross effects of the reliability among each other. This is out of the scope of this paper.

B. Experimental Results (Converter Power Losses)

Although mission profiles of high accuracy are available for power electronics applications, the junction temperature measurement under full loading condition is still challenging and it is an ongoing topic [28]. As the thermal performance of the power devices is coupled with the electrical behavior through

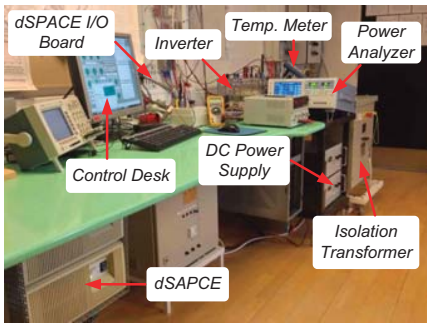

Fig. 12. Experimental setup of a single-phase single-stage 3 kW PV inverter system.

power losses, in case that the PV system is operating with MPPT-CPG control, the temperature loading can be reflected by the power losses on the power devices. This paper therefore measures the power device losses in a single-stage commercial PV inverter and also the case temperature under different input power levels, in order to reveal the relationship between power device losses and the junction temperature. Consequently, the reduced thermal loading (i.e. improved reliability) enabled by the MPPT-CPG control scheme is indirectly verified.

In those dSPACE control system based experiments, the power losses were measured using a YOKOGAWA WT3000 Precision Power Analyzer. The case temperature was recorded through a precise temperature meter. A commercial DC power supply was adopted, and the DC link voltage was set to be v_{dc} = 450 V to ensure the power injection. A PR current controller (k_{pr} = 8, k_{ir} = 2000) was adopted and a repetitive controller [29] was used to compensate the harmonics. The system parameters are the same as those in the simulations except that an LC filter was used in the experiments. The values of the inductor and capacitor are L_i = 3.6 mH and C_f = 2.35 μF, respectively. The system is connected to the grid through an isolation transformer with the leakage inductance of L_g = 4 mH, as shown in Fig. 12.

Fig. 13 shows the performance of the PV inverter under different power levels through the tests. It can be seen in Fig. 13 that the current controller with the repetitive control based harmonic compensator is able to ensure the current injection with a satisfactory power quality under different power levels. However, the power losses of the power switching devices are different in those cases and thus the junction temperature of the power switching devices, which has been verified by the results shown in Fig. 14. It has been confirmed that the total power losses of the power devices increase with the input power levels, and thus the case temperature and the junction temperature. Due to the large thermal capacitance from the case to the heat-sink, although a sudden power change (e.g. the PV output power variation) will lead to a fast response of the power losses on the power switching devices, the case temperature takes a longer time to come into steady-state. However, this is not the case for the junction temperature, as the junction of the power device has a much smaller time-

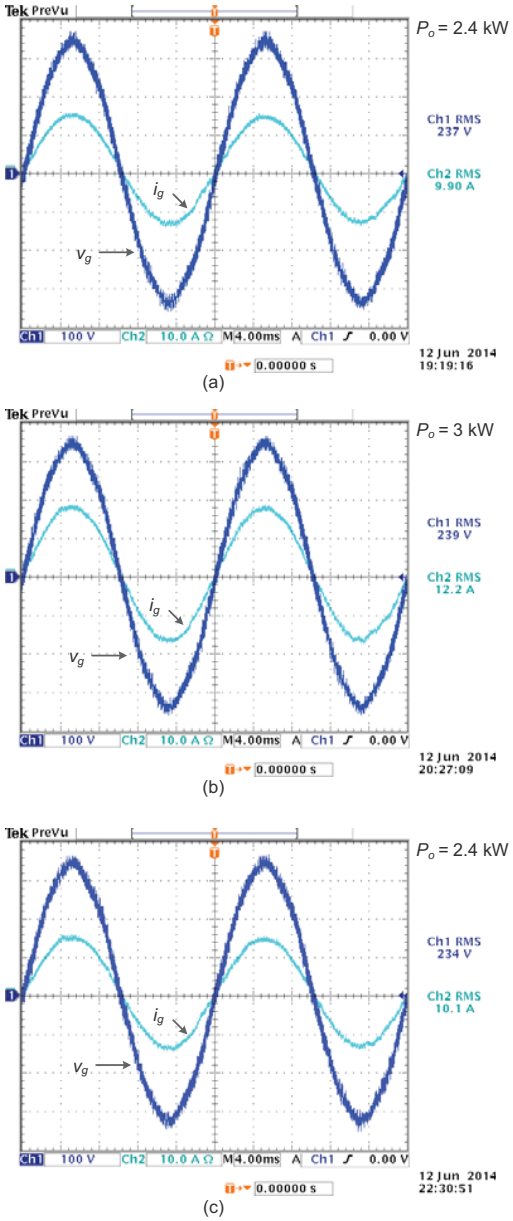

Fig. 13. Performance of a single-phase single-stage PV inverter system operating at unity power factor under different power levels (grid voltage: v_g [100 V/div], grid current: i_g [10 A/div], time [4 ms/div]): (a) P_o = 2.4 kW at 19:19, (b) P_o = 3 kW at 20:27, and (c) P_o = 2.4 kW at 22:30.

constant. Therefore, a sudden power losses change will contribute a prompt junction temperature response. Nevertheless, for both short-term and long-term operations, the MPPT-CPG control is able to reduce the thermal loading of the power devices, and thus improve the reliability.

V. Conclusion

The feasibility to improve the reliability of power devices (e.g. IGBTs) in single-phase PV inverters by limiting the maximum feed-in power has been explored in this paper. A hybrid MPPT-CPG control scheme has been applied to fulfill

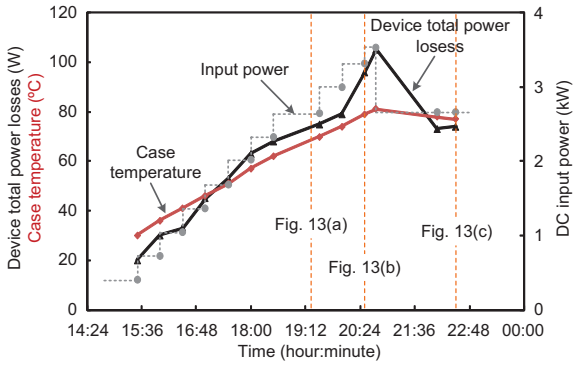

Fig. 14. Total power losses and case temperature of the power devices in a single-phase single-stage PV inverter system under different power levels.

the power limiting function. A time-efficient mission profile based reliability analysis approach has been extended and adopted to predict the lifetime of power devices by considering the temperature loading profiles due to both long-term varying operating conditions and short-term fundamental frequency varying power losses. The proposed control scheme and the extended reliability analysis method have been applied on a 3 kW single-phase PV inverter. The simulation results reveal that, besides the peak power limiting function, the CPG control could extend the lifetime to 2.86 times and 5.62 times for the devices of the PV inverters, respectively, when the maximum power is limited to 90 % and 80 % of the rated one. Moreover, the corresponding energy yield reductions are of 3.11 % and 6.23 %, respectively. This penalty is economically viable since it avoids large investment in expanding the grid capacity and reduces the cost due to PV inverter failures. The quantitative study performed in this paper provides a guidance on the trade-off between the lifetime extension and the yearly energy generation. Besides, experimental testing results have demonstrated the relationship between input power levels and the case temperature, which implies the reliability improvement enabled by the limiting maximum feed-in power control.

REFERENCES

[1] D. Rosenwirth and K. Strubbe, "Integrating variable renewables as Germany expands its grid," *RenewableEnergyWorld.com*. [Online]. Available: http://www.renewableenergyworld.com/, Mar. 2013.

[2] Z. Shahan, "Solar PV market 2014 - 7 predictions," [Online]. Available: http://www.abb-conversations.com/2014/01/, 6 Jan. 2014.

[3] Fraunhofer ISE, "Recent facts about photovoltaics in Germany," Fraunhofer Institute for Solar Energy Systems, Germany, Tech. Rep., [Online]. Available: http://www.abb-conversations.com/2014/01/, 28 May, 2014.

[4] H. Gaztanaga, J. Landaluze, I. Etxeberria-Otadui, A. Padros, I. Berazaluce, and D. Cuesta, "Enhanced experimental PV plant grid-integration with a MW Lithium-Ion energy storage system," in *Proc. of ECCE'13*, pp. 1324-1329, 15-19 Sept. 2013.

[5] F. Blaabjerg and K. Ma, "Future on power electronics for wind turbine systems," *IEEE Journal of Emerging and Selected Topics in Power Electronics*, vol. 1, no. 3, pp. 139–152, Sept. 2013.

[6] A. Hoke and D. Maksimovic, "Active power control of photovoltaic power systems," in *Proc. of SusTech'13*, pp. 70-77, 2013.

[7] Y. Yang, P. Enjeti, F. Blaabjerg, and H. Wang, "Suggested grid code modifications to ensure wide-scale adoption of photovoltaic energy in distributed power generation systems," in *Proc. of IEEE-IAS Annual Meeting*, pp. 1-8, 6-11 Oct. 2013.

[8] A. Ahmed, L. Ran, S. Moon, and J.-H. Park, "A fast PV power tracking control algorithm with reduced power mode," *IEEE Trans. Energy Conversion*, vol. 28, no. 3, pp. 565–575, Sept. 2013.

[9] Y. Yang, F. Blaabjerg, and H. Wang, "Constant power generation of photovoltaic systems considering the distributed grid capacity," in *Proc. of IEEE APEC'14*, pp. 379-385, Mar. 2014.

[10] T. Stetz, F. Marten, and M. Braun, "Improved low voltage grid-integration of photovoltaic systems in Germany," *IEEE Trans. Sustain. Energy*, vol. 4, no. 2, pp. 534–542, Apr. 2013.

[11] H. Beltran, E. Bilbao, E. Belenguer, I. Etxeberria-Otadui, and P. Rodriguez, "Evaluation of storage energy requirements for constant production in PV power plants," *IEEE Trans. Ind. Electron.*, vol. 60, no. 3, pp. 1225–1234, Mar. 2013.

[12] H. Wang, M. Liserre, and F. Blaabjerg, "Toward reliable power electronics: Challenges, design tools, and opportunities," *IEEE Ind. Electron. Mag.*, vol. 7, no. 2, pp. 17–26, Jun. 2013.

[13] H. Huang and P. Mawby, "A lifetime estimation technique for voltage source inverters," *IEEE Trans. Power Electron.*, vol. 28, no. 8, pp. 4113–4119, Aug. 2013.

[14] A.T. Bryant, P.A. Mawby, P.R. Palmer, E. Santi, and J.L. Hudgins, "Exploration of power device reliability using compact device models and fast electro-thermal simulation," *IEEE Trans. Ind. Appl.*, vol. 44, no. 3, pp. 894–903, May-Jun. 2008.

[15] M. Musallam and C.M. Johnson, "An efficient implementation of the rain-flow counting algorithm for life consumption estimation," *IEEE Trans. Reliability*, vol. 61, no. 4, pp. 978–986, Dec. 2012.

[16] I.F. Kovačević, U. Drofenik, and J.W. Kolar, "New physical model for lifetime estimation of power modules," in *Proc. of IPEC 2010*, pp. 2106-2114, Jun. 2010.

[17] Y. Yang, H. Wang, F. Blaabjerg, and K. Ma, "Mission profile based multi-disciplinary analysis of power modules in single-phase transformerless photovoltaic inverters," in *Proc. of EPE'13 ECCE Europe*, pp. 1-10, 2-6 Sept. 2013.

[18] S. Harb and R.S. Balog, "Reliability of candidate photovoltaic module-integrated-inverter (PV-MII) topologies - A usage model approach," *IEEE Trans. Power Electron.*, vol. 28, no. 6, pp. 3019–3027, Jun. 2013.

[19] S.E. De León-Aldaco, H. Calleja, F. Chan, and H.R. Jiménez-Grajales, "Effect of the mission profile on the reliability of a power converter aimed at photovoltaic applications - A case study," *IEEE Trans. Power Electron.*, vol. 28, no. 6, pp. 2998–3007, Jun. 2013.

[20] M. Denk and Mark-M. Bakran, "Efficient online-algorithm for the temperature cycle recording of an IGBT power module in a hybrid car during inverter operation," in *Proc. of CPIS 2014*, pp. 1-6, Feb. 2014.

[21] U. Scheuermann, "Pragmatic bond wire model," *ECPE Workshop*, 3-4 Jul. 2013.

[22] A. Wintrich, U. Nicolai, W. Tursky, and T. Reimann, *Application manual power semiconductors*. Nuremberg: ISLE-Verlag, 2011.

[23] F. Blaabjerg, R. Teodorescu, M. Liserre, and A.V. Timbus, "Overview of control and grid synchronization for distributed power generation systems," *IEEE Trans. Ind. Electron.*, vol. 53, no. 5, pp. 1398–1409, Oct. 2006.

[24] M. Ciobotaru, R. Teodorescu, and F. Blaabjerg, "Control of single-stage single-phase PV inverter," in *Proc. of EPE'05*, pp. P.1-P.10, 2005.

[25] H. Wang, M. Liserre, F. Blaabjerg, P. de Place Rimmen, J.B. Jacobsen, T. Kvisgaard, and J. Landkildehus, "Transitioning to physics-of-failure as a reliability driver in power electronics," *IEEE Journal of Emerging and Selected Topics in Power Electronics*, vol. 2, no. 1, pp. 97–114, Mar. 2014.

[26] A. Aal, "A new rainflow - Free method to transfer irregular load mission profile data into appropriate lab test conditions for design optimization," in *Proc. of CPIS 2014*, pp. 1-6, Feb. 2014.

[27] K. Ma, M. Liserre, F. Blaabjerg, and T. Kerekes, "Thermal loading and lifetime estimation for power device considering mission profiles in wind power converter," *IEEE Trans. Power Electron.*, vol. PP, no. 99, pp. 1–14, early access 2014.

[28] Y. Avenas, L. Dupont, and Z. Khatir, "Temperature measurement of power semiconductor devices by thermo-sensitive electrical parameters - A review," *IEEE Trans. Power Electron.*, vol. 27, no. 6, pp. 3081–3092, Jun. 2012.

[29] Y. Yang, K. Zhou, and F. Blaabjerg, "Harmonics suppression for single-phase grid-connected PV systems in different operation modes," in *Proc. of IEEE APEC'13*, pp. 889-896, Mar. 2013.